Mutual Influence between Reaction-Induced Phase Separation and Isothermal Crystallization in POM/Epoxy Resin Blends

Sara Goossens and Gabriël Groeninckx*

Laboratory of Macromolecular Structural Chemistry, Department of Chemistry, Division of Molecular and Nanomaterials, Katholieke Universiteit Leuven, Celestijnenlaan 200F, 3001 Heverlee, Belgium

Received June 23, 2006; Revised Manuscript Received August 3, 2006

ABSTRACT: The phase morphology development in blends of DGEBA/POM/DDS was studied at cure temperatures below the melting temperature of POM, namely 150, 145, and 140 °C. The phase separation behavior of the blends varying from 5 up to 30 wt % POM was examined with OM, SALLS, and SEM. Different demixing mechanisms were observed depending on the blend composition. Curing at 150 °C induced RIPS followed by crystallization inside the POM-rich matrix phase. When cured at 145 °C, all blends showed spherulitic crystallization starting before the RIPS. This resulted in a gradient of phase-separated structures. It has been shown that increasing the nucleation density could suppress the interspherulitic demixing. This has been realized by changing the thermal history of the thermoplastic in the blends or by lowering the cure temperature to 140 °C. Moreover, the intraspherulitically segregated epoxy resin continued to cure and generated a "spherulite-like" morphology. Next, the spherulite growth rate of POM at 150 and 145 °C was determined for blends cured for 4 h at 180 °C, for blends cured at 150 and 145 °C, and finally for blends without hardener. Curing the epoxy resin favors the crystallization rate of POM in the blends. Depending on the cure temperature and blend composition, different spherulite growth rates were observed. The fastest growth rate was observed for the blends cured at 180 °C and the slowest growth rate for the blends without hardener.

1. Introduction

Polyoxymethylene (POM, polyacetal) is a semicrystalline engineering thermoplastic polymer, which has excellent physical and mechanical properties but is insoluble in most solvents. Blending it with an epoxy resin gives a homogeneous mixture before curing starts, since POM is soluble with the epoxy monomer. During isothermal curing phase separation may occur due to the increase of the molar mass of the epoxy resin, which results in a thermodynamically unstable system. This is translated in a shift of the phase diagram. Dependent on the position of the blend in the phase diagram, phase separation can occur via spinodal decomposition (SD) or nucleation and growth (NG).[1−9] During spinodal decomposition a cocontinuous structure is formed, which can break up in small particles dispersed in a matrix. SD occurs at or close to the critical point, where small concentration fluctuations lead to demixing. At off-critical regions phase separation occurs through nucleation and growth; in this case large concentration fluctuations are necessary for phase separation.

One of the most important analysis techniques for the study of the demixing mechanism is light scattering. Depending on the size scale of the phases formed, laser light (SALLS),[3,10−12] visible light (OM),[5,13] or a combination of both[6,14] is used. SD is characterized in SALLS through the appearance of a diffraction ring, which increases in intensity and decreases in diameter throughout the phase separation process. In general, the intensity increase reflects the difference in refractive indices between the phases, whereas the contraction of the ring to smaller angles reflects the growth of the phases. In conventional studies often the same dynamics for the two components in a thermosetting blend are assumed, although the size of the molecules involved at the beginning of the phase separation process is clearly different. This is called "dynamic asymmetry". This asymmetry induces unusual phase morphologies like the spongelike phase-inversed structure and the moving droplet phase.[15−18] This so-called viscoelastic phase separation was first reported by Tanaka et al.[19] and has been observed in the POM/epoxy system used.[20]

In initially homogeneous blends, where one component is semicrystalline and the other one is amorphous, curing not only leads to reaction-induced phase separation (RIPS), but depending on the temperature, isothermal crystallization can interfere. Semicrystalline modifiers like ϵ-polycaprolactone (PCL),[21,22] poly(butylene terephthalate) (PBT),[23,24] and syndiotactic polystyrene (sPS)[25,26] have been used before. Crystallization in thermosetting blends containing a crystallizable thermoplastic component will be greatly affected by the miscibility, the phase behavior and morphology of the cross-linked blends, and the topological effect of the network.[22,27−31]

This study of the POM/epoxy system describes how the variation of the cure temperature leads to the development of different phase morphologies, each displaying their own crystallization kinetics. Using POM as modifier allows to investigate the different possibilities, namely crystallization before or after RIPS, i.e., crystallization in a homogeneous or phase-separated blend. In a previous paper[20] three different cure conditions were discussed, each leading to a different phase morphology. In this paper crystallization at different cure temperatures below the melting point of POM will be examined. Systematically, the cure temperature will be changed from 150 to 145 and 140 °C, which will alter the starting order of RIPS and crystallization. Moreover, both processes will influence each other, which will lead to complex blend morphologies.

2. Experimental Section

2.1. Materials. The epoxy resin used is a low molar mass liquid diglycidyl ether of bisphenol A (DGEBA) (Epikote 828VEL, EEM 182−187 g, ICI, Belgium) with an epoxide equivalent weight of 5.36 mol/kg. The hardener used was 4,4′-diaminodiphenyl sulfone (DDS) (Sigma-Aldrich, A7, 480−7, M_w = 248 g/mol), and the

* Corresponding author: e-mail gabriel.groeninckx@chem.kuleuven.be; tel +32-16-327440; fax +32-16-327990.

10.1021/ma061415t CCC: $33.50
Published on Web 10/17/2006

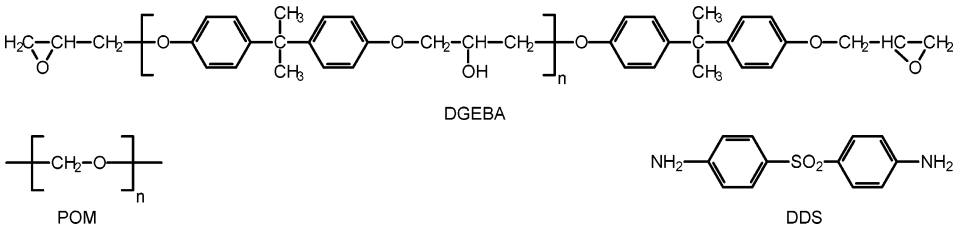

Figure 1. Chemical structures of DGEBA, DDS, and POM.

Table 1. Overview of Onset Times of the Reaction-Induced Phase Separation and Isothermal Crystallization for Different Blends at Different Cure Temperatures

wt % POM	RIPS (min) 180 °C[a]	RIPS (min) 150 °C[a]	isothermal crystallization (min)	RIPS (min) 145 °C[a]	isothermal crystallization (min)
5	10.2	28.9		32.6	22
10	10.5	30.2		33.7	17
15	10.4	29.2	41.4	36.1	16
20	12.1	31.4	45	35.9	10
30	12.6	34.8	55	37	9

[a] Cure temperature.

crystallizable thermoplastic component is polyoxymethylene (POM) (Hostaform C9021 naturel, $T_m = 168$ °C, $T_c = 138$ °C), modified with a sterical hindered phenol, used as antioxidant. The end groups were modified with the comonomer dioxolane as to increase the thermal stability. POM was kindly provided by Ticona, Benelux. The chemical structures of DGEBA, DDS, and POM are given in Figure 1.

2.2. Sample Preparation. The blend preparation occurred in three steps. First, the thermoplastic component was added to the epoxy monomer at 180 °C under stirring until a homogeneous mixture was obtained. Next, DDS was added to this mixture in the stoichiometric ratio of epoxy to amino hydrogens equal to 1 under continuous stirring for ~30 s. Finally, the mixture was quenched for 1 min in liquid nitrogen to minimize the epoxy conversion before the actual measurements started. Blends of 5, 10, 15, 20, and 30 wt % POM were prepared with melt-mixing.

2.3. Techniques. *2.3.1. Optical Microscopy.* Optical microscopy (OM) was used to investigate the behavior of the DGEBA/POM/DDS blends visually. Measurements were performed on an Olympus BH_2 microscope equipped with cross-polarizers. Samples of several milligrams were put between two glass slides and placed in a Mettler FP82-HT hot stage. Digital micrographs were taken at several cure times by a JVC TK-C1381 CCD camera and analyzed by the program Qwin of Leica Co. During isothermal measurements at 150 and 145 °C the phase separation and isothermal crystallization of POM were studied.

To calculate the crystallization growth rates, spherulite radii were determined as a function of time and converted into spherulite growth rates using a script within the Leica Qwin Image Analysis software program.

2.3.2. Small-Angle Laser Light Scattering. The small-angle laser light scattering (SALLS) setup used comprises a linear polarized 1 mW Spectra-Physics 117A type He−Ne laser ($\lambda = 632.8$ nm), a polarizer set parallel to the laser polarization, the sample in a Mettler FP-82HT hot stage, a second polarizer (analyzer), a screen with a beam catcher on which the scattering patterns are projected, and a Photometrix ATC200L cooled CCD camera as detector. The scattering angles were calibrated using a 100 lines/mm grid. Samples of a few milligrams were put between two microscope glass slides and placed into the Mettler oven to examine the phase separation process and/or the crystallization. During the measurements the analyzer was placed parallel (Vv setup) or perpendicular (Hv setup) to the polarizer using a flipper. The scattered intensity was recorded as a function of time on a PC. Every 15 s a picture was taken. Processing of the data was performed with a homemade script running under V for Windows (version 3.5b, Digital Optics Ltd.). The software takes care of the integration of the scattered intensities, which results in the relative total light scattering intensity and an azimuthal averaging of the 2D patterns. Analyzing the scattering patterns led to the determination of the onset and mechanism of the phase separation and the onset of crystallization.

2.3.3. Scanning Electron Microscopy. To examine the phase morphology of the different blends, scanning electron microscopy (SEM) was used. SEM pictures were taken with a Philips XL20 Series SEM. At first, the samples were fractured in liquid nitrogen, avoiding deformation at break. Next, they were etched with benzyl alcohol at 136 °C to remove the thermoplastic component POM and finally dried overnight under vacuum to remove any residual solvent. Each sample was coated with a thin gold layer to improve the electron conductivity during the SEM measurements.

3. Results and Discussion

It has been shown in a previous article[20] that varying the blend composition has major consequences for the phase separation process and the resulting blend morphology. When a cure temperature below the melting point of POM is applied, it can be expected that the variation of the POM concentration will also result in different phase morphologies. As a consequence, the study of the phase behavior was performed systematically: the concentration of POM was gradually increased from 5 up to 30 wt % POM, similar to $T_{cure} = 180$ °C. Both OM and SALLS are used in the study of the phase behavior. OM was mainly used to visualize the phase separation process, whereas SALLS was used in order to determine the onset times for RIPS and isothermal crystallization. To destroy the thermal history, all blends were first kept for 1 min at 180 °C before they were cooled to the isothermal cure temperature.

In the previous article,[20] some first results concerning the phase behavior of POM/epoxy blends below the melting temperature of POM were analyzed. Table 1 summarizes the onset times of RIPS and/or isothermal crystallization for the cure temperatures of 180, 150, and 145 °C. In this paper further results concerning the phase behavior of the different blends with 5, 10, 15, 20, and 30 wt % POM, cured at 150, 145, and 140 °C, will be presented in the following sections.

3.1. Phase Separation Followed by Isothermal Crystallization: Curing at 150 °C. Figure 2 displays the OM pictures of the phase separation process of a blend with 10 wt % POM cured at 150 °C, showing an initial cocontinuous structure (Figure 2a), which breaks up into POM-rich droplets dispersed in an epoxy-rich matrix (Figure 2b). These droplets grow in size during the phase separation process (Figure 2c). This morphology coarsening occurs due to ripening: larger droplets develop at the expense of smaller ones and the total number of droplets decreases. A blend with 5 wt % POM exhibits a similar

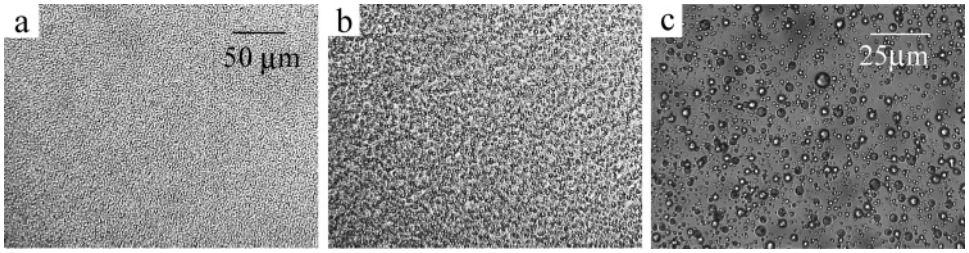

Figure 2. OM pictures of a blend with 10 wt % POM cured at 150 °C for different times: (a) 29, (b) 44, and (c) 120 min.

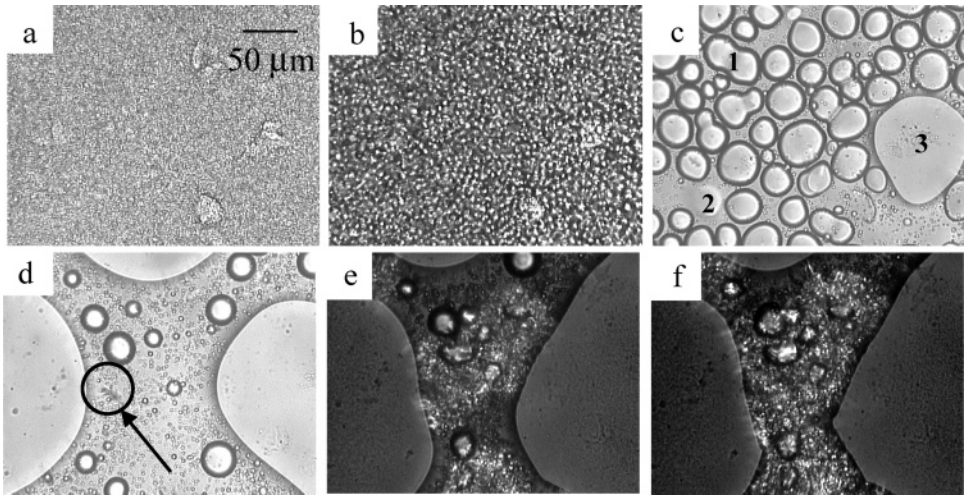

Figure 3. OM pictures of a blend with 20 wt % POM cured at 150 °C for different times: (a) 31, (b) 35, (c) 41, (d) 45, (e) 66, and (f) 71 min.

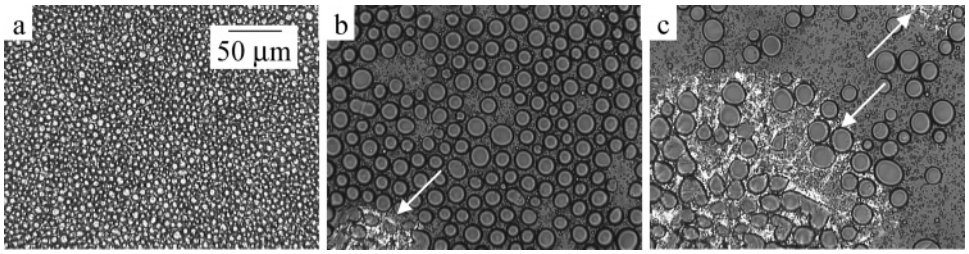

Figure 4. OM pictures of a blend with 30 wt % POM cured at 150 °C for different times: (a) 50, (b) 66, and (c) 92 min.

phase separation behavior: i.e., a change from a cocontinuous structure to a droplet-matrix structure (not shown here). No isothermal crystallization was observed for these blends, since upon cooling homogeneous crystallization sets in around 85 °C, similarly as in the 5 and 10 wt % POM blends cured at 180 °C.[20] The temperature difference between 150 and 85 °C is too large to induce homogeneous crystallization in the dispersed POM-rich droplets.

For a blend with 20 wt % POM, however, isothermal crystallization is observed after phase separation has set in. Figure 3a,b displays an initial cocontinuous structure, indicating spinodal demixing, breaking up into epoxy-rich droplets dispersed in a POM-rich matrix, which coalesce and grow (indicated as droplet 1 in Figure 3c). In the meanwhile the difference in refractive indices between the POM-rich and the epoxy-rich phase becomes smaller because of the polymerization process of the epoxy monomers in the POM-rich phase. This will increase the refractive index of the POM-rich phase (which has the lowest refractive index), approaching the one of the epoxy-rich phase and the epoxy holes disappear (indicated as droplet 2 in Figure 3c). The growing epoxy oligomers in the POM-rich phase, however, will at a given moment be rejected due to a secondary phase separation. Small epoxy-rich particles are generated and the refractive index of the POM-rich matrix phase decreases again, resulting in the reappearance of the large epoxy-rich droplets (indicated as droplet 3 in Figure 3c). The same "apparent phase dissolution" process was observed for a blend with 20 wt % POM, cured at 180 °C.[20] For additional information the reader is referred to this publication. Fifteen minutes after L−L demixing has set in, a growing spherulite can be seen in the POM-rich matrix phase in between the epoxy droplets (Figure 3d). The growing spherulite is indicated with a circle. The last two pictures are taken with partially crossed polarizers in order to focus on the spherulites (Figure 3e,f).

A similar phase separation behavior and subsequent isothermal crystallization have been observed for a blend with 15 wt % POM (not shown here). This blend displays a phase-inverted structure when cured at 150 °C but a cocontinuous structure when cured at 180 °C.[20]

The growth of the spherulites in the POM-rich matrix can also nicely be observed during the phase separation process of a 30 wt % POM blend, cured at 150 °C. First, a transition from a cocontinuous structure to a droplet-matrix structure is observed (Figure 4a). Next, the apparent phase dissolution as well as the isothermal crystallization is shown in Figure 4b,c, which are taken with partially crossed polarizers. In these pictures the growth fronts of the spherulites are indicated with arrows. The droplets shown in Figure 4 consist of the epoxy-rich phase; the matrix consists of the POM-rich phase, where consequently the isothermal crystallization occurs.

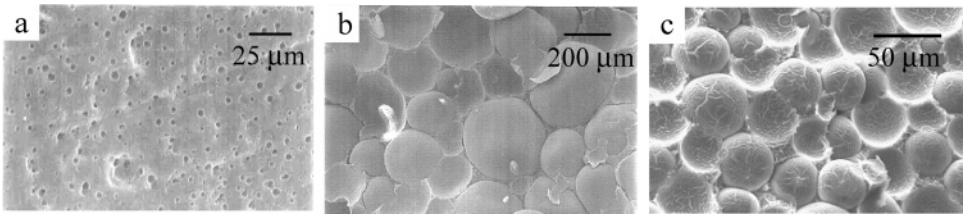

Figure 5. SEM pictures of blends with (a) 10 wt % POM, (b) 15 wt % POM, and (c) 30 wt % POM, cured for 2 h at 150 °C. The POM-rich phase has been etched away.

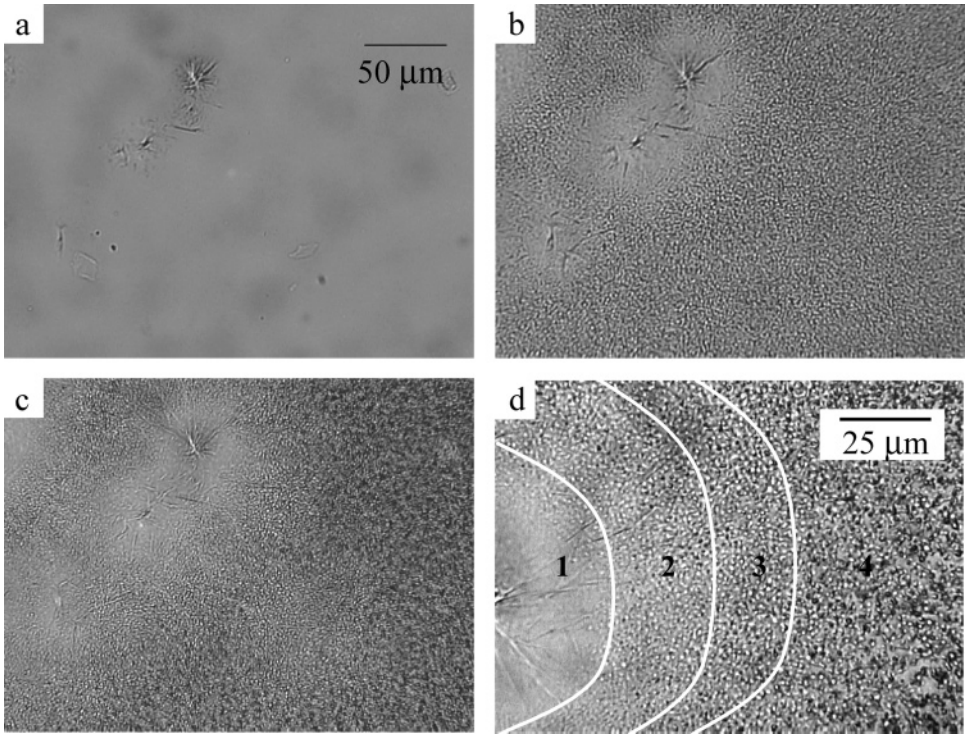

Figure 6. OM pictures of a blend with 5 wt % POM cured at 145 °C for different times: (a) 29, (b) 33, and (c) 60 min. Picture d is an enlargement of a part of picture c.

For the blends with 5 up to 15 wt % POM, a more or less constant onset time of RIPS at 150 °C is obtained (Table 1). Adding more POM increases the onset time due to the dilution of the reactive groups and the formation of nonreactive complexes between the OH groups of the epoxy resin and the ether groups of the thermoplastic.[32] Compared to the onset times of RIPS at 180 °C, those of the blends cured at 150 °C are larger since the reaction rate is slowed down at lower temperatures. The onset time of isothermal crystallization has a minimum at 15 wt % POM and increases with increasing amount of POM due to a more pronounced partial miscibility, which can be derived from the occurrence of the "apparent phase dissolution". For the same reason, the time difference between RIPS and isothermal crystallization increases with increasing amount of POM. Blends with 5 and 10 wt % POM did not show isothermal crystallization of POM at 150 °C. Obviously, crystallization in the small droplets needs to be induced homogeneously, and this only happens at a large degree of supercooling. However, all blends demix according to the spinodal mechanism, each displaying a cocontinuous structure at the beginning of RIPS. Depending on the blend composition, different blend morphologies are generated.

The final morphologies of three blend systems are displayed in Figure 5 as SEM pictures of different blends cured for 2 h at 150 °C. Blends with 5 and 10 wt % POM have a particle/matrix structure with the epoxy-rich phase as matrix (Figure 5a). Larger droplets are observed with the blend of 10 wt % POM because of the larger amount of POM present. Blends containing 15 up to 30 wt % POM have a phase-inverted structure (Figure 5b,c); the higher the amount of POM, the smaller the epoxy holes are. Increasing the amount of POM increases the viscosity of the matrix phase, which makes coalescence more difficult, and consequently smaller epoxy particles are formed.

Finally, it can be concluded that in general at $T_{cure} = 150$ °C a similar phase morphology development is encountered compared to $T_{cure} = 180$ °C.[20] The occurrence of isothermal crystallization in the POM-rich matrix phase for blends with 15 up to 30 wt % POM does not alter the phase separation process much.

3.2. Isothermal Crystallization Followed by Phase Separation: Curing at 145 °C. Similar to the blends cured at 150 °C, the phase separation and the occurrence of isothermal crystallization were investigated with mainly OM and SALLS. Blends with compositions varying from 5 up to 30 wt % POM were first kept for 1 min at 180 °C to melt the POM present and then cooled at 40 °C/min to 145 °C, where they were cured isothermally.

Starting with a blend with 5 wt % POM, Figure 6 displays the phase separation process at 145 °C. A whole different phase development is observed compared to the blends cured at 180 and 150 °C, where a particle/matrix structure was formed. Here, isothermal crystallization starts before the liquid−liquid phase separation, as caused by the cure reaction of the epoxy resin. In chronological order the phase development can be described

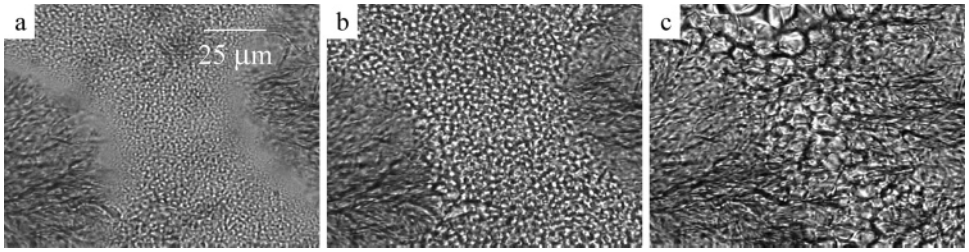

Figure 7. OM pictures of a blend with 15 wt % POM cured at 145 °C at different times: (a) 37, (b) 38, and (c) 42 min.

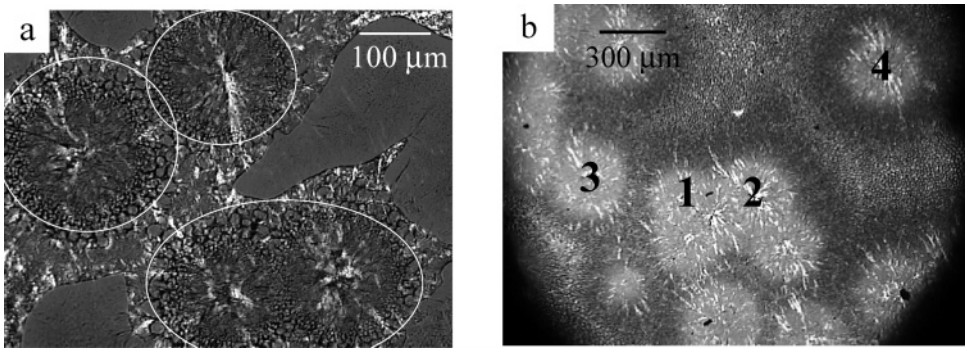

Figure 8. OM pictures of (a) a 15 wt % POM blend and (b) a 30 wt % POM blend cured for 1 h at 145 °C.

as follows: after 22 min, small spherulites are formed in the homogeneous blend (Figure 6a). At this moment, the conversion degree of pure epoxy is 17%, which will not differ much with the 5 wt % POM blend. In this relatively low viscous blend, the POM molecules are able to diffuse toward one another and will form a stable nucleus. After 33 min, the interspherulitic zone starts to phase separate and a cocontinuous structure is formed (Figure 6b). This cocontinuous structure breaks up in small POM-rich droplets dispersed in an epoxy-rich matrix (Figure 6c) after 3 or 4 min of curing (difficult to observe due to the small scale of the phase separation process). These small POM-rich droplets do not crystallize at the applied cure temperature. Indeed, they can be compared with the small POM-rich droplets formed in the 5 and 10 wt % POM blends cured at 180 °C, which crystallize dynamically around 85 °C.[20] While the L−L phase separation is going on, the spherulites continue to grow through the POM-rich continuous part of the cocontinuous structure. Once they reach the particle/matrix structure, the crystallization will stop, as POM has to diffuse in the highly viscous epoxy-rich matrix toward the growth front. Figure 6d shows a gradient in the phase-separated structure next to the spherulite in a blend with 5 wt % POM. The spherulite is divided in three zones, depending on the environment in which the spherulite grew. Zone 1 represents the spherulite growth in the homogeneous sample, where no RIPS occurred yet. Next, zone 2 depicts the spherulite growth in the cocontinuous structure, and finally zone 3 displays the growth of the spherulite in the particle/matrix structure. As said before, the growth of the spherulite in zone 3 is limited because of the slow diffusion of very diluted POM molecules in the epoxy-rich matrix. As a result, zone 4 represents the volume which has been phase-separated but did not undergo crystallization at 145 °C. During the crystallization process POM is extracted from the amorphous layer around the growing spherulites. As a consequence, phase separation starts in the volumes distant from the spherulites, since in this zone a relatively large amount of POM is still present. Volumes closer to the crystallization growth front demix later. Accordingly, inspection of the phase-separated structure along the growth path of the spherulites reveals a time gradient of different phase-separated structures with more evolved phase-separated morphologies at larger distances from the center of the spherulites. Moreover, when the spherulite sweeps through the phase-separated structure, the phase morphology development is arrested. Similar results were obtained for the blend with 10 wt % POM but will not be shown here. This trend has been observed previously in nonreactive blends of polypropylene and ethylene−propylene random copolymer by Inaba et al.[33]

Increasing the amount of POM in the blends will change the L−L demixing in the interspherulitic region: the cocontinuous structure will break up in a phase-inverted structure instead of a particle/matrix structure. Figure 7 shows the phase separation of a blend with 15 wt % POM cured at 145 °C. The growth of the spherulites in the homogeneous blend is not shown. The L−L phase separation occurring between the growing spherulites evolves from a cocontinuous structure (Figure 7a) to epoxy-rich droplets dispersed in the POM-rich phase (Figure 7b,c). The epoxy-rich droplets are situated in the middle of the OM pictures b and c. The isothermal crystallization continues through the interspherulitic POM-rich phase while locking in the epoxy-rich droplets. When the phase morphology is examined at a smaller magnification, the OM picture in Figure 8a is obtained. The different spherulites "centers" (i.e., the initially formed spherulites) are indicated with a circle. The birefringence points to crystallization of POM through the whole sample, as the POM-rich phase forms the matrix phase of the liquid−liquid (L−L) phase-separated structure. At smaller magnification it becomes clear that RIPS in the interspherulitic zone has reached the stadium of the apparent phase dissolution and the reappearance of the epoxy-rich holes. As has been discussed above, RIPS starts in zones distant from the spherulites. So the large epoxy holes are located relatively far away from the center of the spherulites and display secondary phase separation.

Increasing the amount of POM even further, a similar phase separation behavior is encountered for the blends with 20 wt % POM (not shown) and 30 wt % POM. As for the 15 wt % POM blend, in between the growing spherulites, L−L phase separation occurs with the formation of a cocontinuous structure, which evolves to a phase-inverted structure displaying epoxy-rich droplets. Figure 8b shows the morphology after 1 h of curing at 145 °C for a 30 wt % POM blend. Increasing the concentration of POM in the blends results in a higher nucleation density and an increased crystallization growth rate (see also

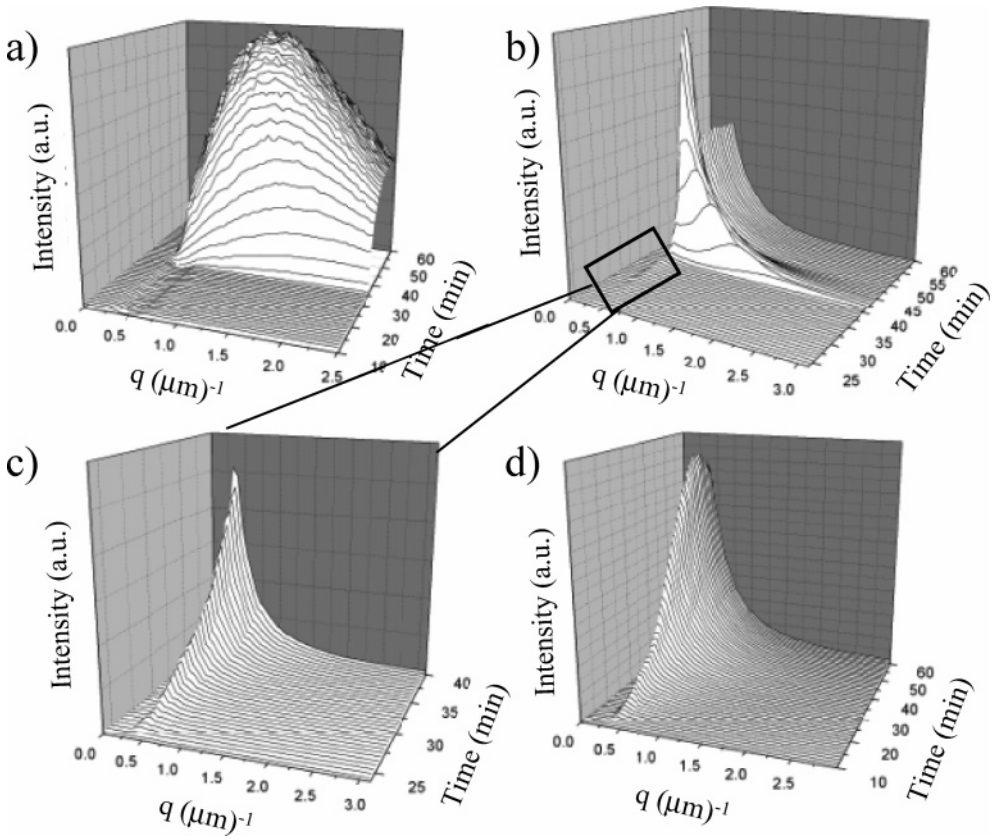

Figure 9. Scattering patterns obtained with SALLS for blends with (a) 5 wt % POM, (b, c) 15 wt % POM, and (d) 30 wt % POM cured at 145 °C. Picture c is a magnification of picture b.

section 3.4), which will influence the RIPS in the interspherulitic zone. It can be seen that the spherulites grown in the homogeneous sample (bright areas in Figure 8b) are larger for the 30 wt % POM blend compared to the 15 wt % POM blend. The dark circles surrounding these spherulites in Figure 8b correspond to the crystallization in the cocontinuous phase-separated structures and in the POM-rich matrix, which contains very small epoxy-rich droplets. For the 30 wt % POM blend, however, the L−L phase separation cannot reach the stage of apparent phase dissolution, as was the case for the 15 wt % POM blend, due to the high nucleation density and crystallization rate. It can also be seen that the position of the spherulites determines the stage of RIPS that will be reached locally. Spherulites 1 and 2 meet each other before RIPS starts, and hence no phase-separated structures can be seen between them. The spherulite centers 1 and 3 are closer to each other than those of spherulites 1 and 4, and consequently the phase-separated structures between the latter are more evolved.

Next, the small-angle laser light scattering (SALLS) patterns of the blends cured at 145 °C will be discussed, referring to the OM pictures, displayed above. Few spherulites are formed in a blend with 5 wt % POM, and as a consequence the L−L demixing can be clearly observed in the scattering experiments since the spherulites are not volume filling (Figure 9a). The growth of the cocontinuous structure occurs very slowly, corresponding to the SALLS scattering peak moving slowly to smaller angles. Afterward, the POM-rich particles are formed and the peak will broaden, but that morphology change is occurring after 50 min of curing and as a result cannot be seen. The demixing behavior of a blend with 15 wt % POM is a nice example of the superposition of the scattering intensities of both phenomena. Figure 9b shows the total Vv scattering profile of the blend. At first sight, only the phase separation scattering is visible as a small peak appearing at large angles, which shifts to smaller angles with time and finally disappears behind the beam stop. This scattering peak is related to the growth of the cocontinuous structure, which is coarser than in the blends with 5 and 10 wt % POM. This results in a scattering peak at lower q values. When the scattering data before the appearance of the scattering peak are enlarged (Figure 9c), a clear increase of the scattering intensity around the beam stop can be seen, indicating the growth of the spherulites which scatter more as they grow in number and size. Very clearly, most of the spherulite scattering occurs behind the beam stop. For blends with 30 wt % POM (Figure 9d), the crystallization spreads out through the whole sample, making the observation of both processes with SALLS impossible.

In Table 1, a decrease of the onset time of crystallization at 145 °C is observed with increasing POM content, as expected both from kinetic and thermodynamic considerations. The lower the dilution of the crystallizable species, the higher the crystallization rate will be because less foreign species need to migrate away from the crystal growth front and the diffusion of the crystallizable species toward the growth front is facilitated. Second, the depression of the equilibrium melting point decreases with an increase of the concentration of the crystallizable polymer. Accordingly, the supercooling increases with increasing POM concentration in the blends for crystallization at a given temperature. Compared to the onset times of RIPS at $T_{cure} = 150$ °C, a small increase in onset time is seen here. A decrease in cure temperature results in a decrease of the reaction rate of the cure process, thus resulting in a slower increase of the molar mass of the epoxy resin. Although the isothermal crystallization is depleting the amorphous zone with POM, there are still differences in onset time between the different blend compositions, indicating that an initial higher

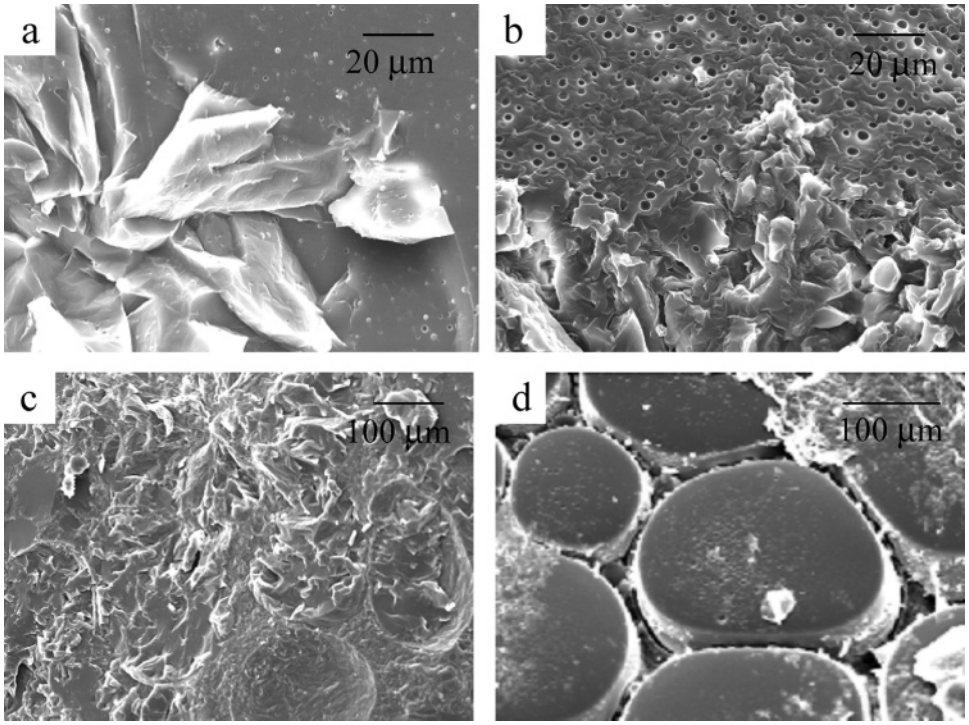

Figure 10. SEM pictures of blends cured for 2 h at 145 °C: (a) 5 wt % POM, (b) 10 wt % POM, (c) 15 wt % POM, and (d) 20 wt % POM. Both phases are visible.

concentration of POM still remains at the moment of RIPS. For a blend with 30 wt % POM for example, the isothermal crystallization will start earlier compared to a blend with 5 wt % POM, as described above, but in the interspherulitic zone relatively more POM remains present than for the 5 wt % POM blend, slowing down the cure reaction, and this will finally result in a larger onset time for the 30 wt % POM blend.

Figure 10 shows the blend morphologies, as observed with SEM, after 2 h of curing at 145 °C, without etching the POM, so that both phases can be clearly observed. Blends with 5 and 10 wt % POM show nicely the spherulites embedded in the phase-separated epoxy-rich matrix. The tiny droplets visible contain the POM-rich phase (Figure 10a,b). The blends containing 15, 20, and 30 wt % POM display a phase-inverted structure, in which the spherulites continue to grow. As a result, it becomes quite difficult to observe the epoxy holes with SEM when POM is not etched away. For the 15 wt % POM blend this is still possible (Figure 10c), but for the 20 and 30 wt % POM blends, this becomes rather difficult. The few epoxy-rich holes, which can be seen, display tiny POM-rich droplets, resulting from the secondary phase separation (Figure 10d).

Up to now, the thermoplastic component was melted for 1 min at 180 °C before the samples were cooled to the cure temperature (150 and 145 °C). At T_{cure} = 145 °C, it was observed that the spherulites were not volume filling at the moment the phase separation started. In this paragraph it will be investigated whether it is possible to completely eliminate interspherulitic RIPS. In a first attempt, a blend with 20 wt % POM was heated to 165 °C and after 15 s cooled to 145 °C. Spherulites appeared after 9 min of curing, and interspherulitic RIPS started after 38 min. Another thermal treatment is hence required in order to avoid RIPS. In a second attempt, the 20 wt % POM blend was heated to 160 °C and after 15 s cooled to 145 °C. The first spherulites appeared after 6 min of curing and became almost completely volume filling before RIPS could start. Figure 11 shows the blend morphology of a 20 wt % POM blend after 45 min of curing at 145 °C. These measurements

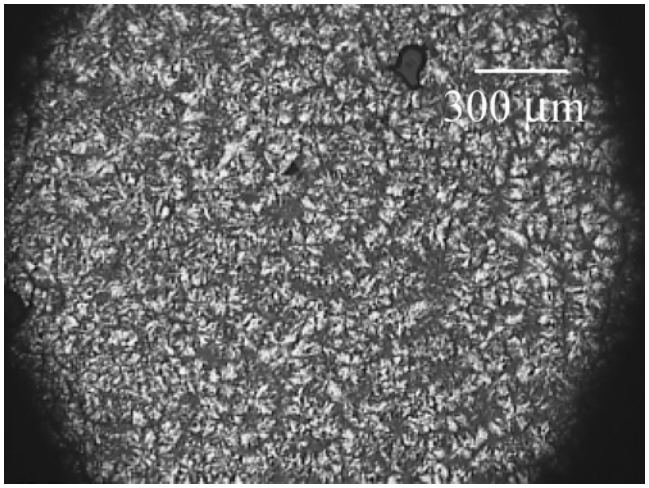

Figure 11. OM picture of a 20 wt % POM cured for 45 min at 145 °C. The blend was first heated to 160 °C and subsequently cooled to 145 °C.

clearly confirm that it is possible to completely exclude reaction-induced phase separation if the nucleation density of the thermoplastic is sufficiently increased. This can be accomplished by changing the thermal history of the blend, i.e., the initial melting of the POM crystallites. A second possibility is to alter the degree of supercooling. This second possibility will be discussed in section 3.3. When the blends are cured at 145 °C, the crystallization will start on heterogeneities present in the sample. These heterogeneities are residues of catalyst, impurities, incomplete melted crystallites, etc. When the number of heterogeneities is increased, more nuclei will form and the sample will crystallize faster. In this blend system, lowering the initial melting temperature can increase the number of nuclei. This will result in more crystallite residues and hence a higher global crystallization rate. The thermal history of the blends is thus crucial for the final blend morphology, since it will

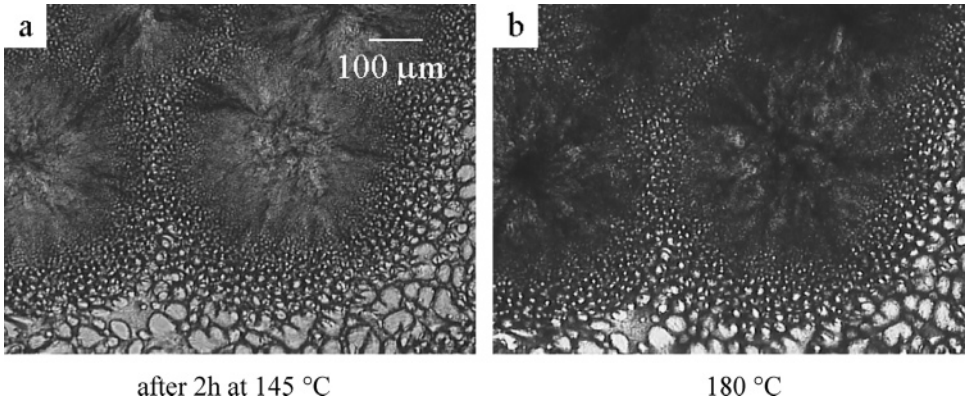

Figure 12. (a) OM pictures of a 20 wt % POM blend cured for 2 h at 145 °C and (b) subsequently heated to 180 °C.

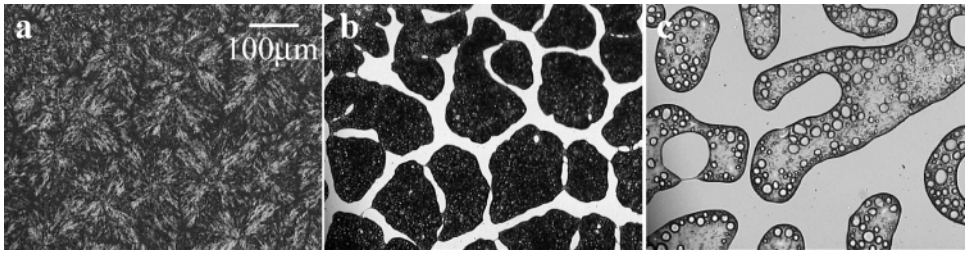

Figure 13. OM pictures of a blend with 20 wt % POM cured for 1 h at 140 °C and subsequently heated again to 180 °C at 10 °C/min: (a) after 1 h at 140 °C, (b) at 160 °C, and (c) after 1 min at 180 °C.

determine whether interspherulitic L−L demixing will occur or not.

It has been shown that spherulites start to grow in the homogeneous sample, followed by interspherulitic L−L demixing, if an appropriate thermal treatment is applied. Since crystallization always includes the segregation of the amorphous component, the question can be asked where the epoxy oligomers are segregated and whether this segregation process stops the cure reaction or not. Next, it will be argued that the cure process continues inside the growing spherulites.

When a 20 wt % POM blend is cured for 2 h at 145 °C and subsequently heated to 180 °C at 10 °C/min, the following observations can be made (Figure 12). After 2 h of curing at 145 °C, it has been observed that the phase morphology consists of spherulites surrounded by a phase-inverted structure (Figure 12a). In the phase-separated POM-rich matrix the crystallization continues and locks in the epoxy-rich droplets. When this structure is heated again, it can be expected that this phase morphology disappears on account of the melting of the spherulites. Nevertheless, the opposite is observed! When 180 °C is reached, an almost identical morphology is visible (Figure 12b). After 2 h of curing at 145 °C, the epoxy conversion has reached 60%, indicating that gelation occurred. Consequently, no coalescence of epoxy droplets upon heating is observed. In the spherulites, on the other hand, the segregated epoxy oligomers also continue to polymerize for 2 h. These growing epoxy chains will adopt a morphology type dictated by the crystallization process, i.e., a spherulite-like morphology. Heating up to 180 °C will make disappear the birefringence, but the spherulite-like morphology still remains! This implies that a large amount of epoxy resin has to be rejected interlamellar or interfibrillar during the crystallization of POM. Real-time SAXS measurements were performed in order to determine the segregation mechanism. The data processing and discussion of the data obtained can be found elsewhere.[34] After 25 min at 145 °C, the amorphous layer thickness is 8.1 nm for the pure POM, 11.1 nm for the 20 wt % POM blend, and 12.0 nm for the 30 wt % POM blend. The larger amorphous layer thickness for the epoxy blends compared to the pure POM points to at least partial interlamellar segregation of the amorphous epoxy component.

3.3. Isothermal Crystallization without Phase Separation: Curing at 140 °C. Another possibility to increase the nucleation density is to change the degree of supercooling. Decreasing the cure temperature to 140 °C will increase the supercooling and consequently the nucleation density.

When a blend with 20 wt % POM is cured at 140 °C, spherulites appear already after 1 min, which could be expected due to the higher supercooling. After 20 min the spherulites are nearly completely volume filling because of the higher nucleation density and local crystallization rate. This morphology type implies that almost all epoxy resin has to be segregated interlamellar or interfibrillar. Figure 13a displays the blend with 20 wt % POM cured for 1 h at 140 °C, displaying spherulites which are almost completely volume-filling. No L−L phase separation is visible. In between the spherulites a small amorphous zone can be seen (i.e., dark lines around the spherulites) which consists mainly of rejected epoxy resin. Subsequently, the blend is heated to 180 °C at 10 °C/min (Figure 13b,c). Around 160 °C, the spherulites start to melt and simultaneously RIPS occurs rapidly (Figure 13b). This indicates that at least some conversion took place inside the spherulites; otherwise, it would take longer before the phase separation starts. The dark areas represent the melting of the POM-rich phase, and the white area represents the epoxy-rich phase. Reaching 180 °C, a kind of cocontinuous structure is observed with in the POM-rich phase (dark zones) secondary phase separation, leading to epoxy-rich droplets (Figure 13c). Similarly to the phase separation mechanism of the blend with 20 wt % POM cured at 180 °C, the disappearance of the epoxy-rich droplets in the POM-rich matrix can be observed, indicating the progress of the cure reaction in this phase. Also in the epoxy-rich continuous phase small POM-rich droplets appear. Simultaneously, the shape of the POM-rich phase is changing toward a more rounded form, which indicates that the surface tension between the epoxy-rich and POM-rich phase increases.

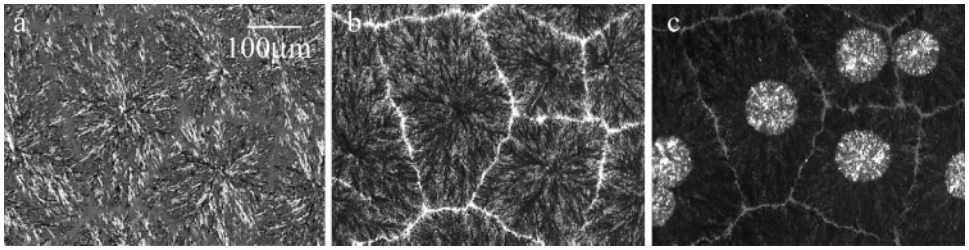

Figure 14. OM pictures of a blend with 20 wt % POM cured for 2 h at 140 °C (a), subsequently heated again to 180 °C at 10 °C/min (b), and finally cooled to 144 °C (c).

Table 2. Overview of the Spherulite Growth Rates in Different Blends and under Different Cure Conditions

	spherulite growth rate at 145 °C (μm/s)					spherulite growth rate at 150 °C (μm/s)	
composition (wt %)	cured 4 h at 180°C	iso 145 °C before PS (1)	iso 145 °C before PS (2)	iso 145 °C after PS	without DDS	cured 4 h at 180 °C	iso 150 °C
5	*a*	0.0331	0.126	0.152	0.0053	*a*	*a*
10	*a*	0.0408	0.136	0.174	0.0112	*a*	*a*
15	7.13	0.0451	0.156	0.224	0.0179	0.592	0.0826
20	8.04	0.0664	0.165	0.275	0.0216	0.631	0.0922
30	7.73	0.112	0.194	0.344	0.0445	0.754	0.133

[a] These blends do not display isothermal crystallization at the applied temperatures, since the POM-rich phase forms the dispersed phase in these particle/matrix structures. Cooling measurements showed dynamic crystallization around 80−90 °C.

When the same experiment is performed, but the isothermal cure time is increased up to 2 h, a completely different result is obtained. Figure 14a represents the spherulites formed after 2 h at 140 °C, which are almost completely volume filling and display birefringence (picture taken with partially crossed polarizers). When heating the sample to 180 °C, the birefringence disappears after melting, but the shape of the spherulites stays intact (Figure 14b: picture taken with *parallel* polarizers). Above the melting temperature of POM a spherulitic morphology thus still exists, similar to the 20 wt % POM blend cured for 2 h at 145 °C. During the crystallization of POM at 140 °C, the epoxy resin has been rejected mainly intraspherulitic. Nevertheless, the segregation in confined spaces did not stop the cure reaction. After 1 h the epoxy resin was not cured enough to fixate the present morphology, but after 2 h it did. For the pure epoxy a conversion degree of 68% is reached; of course, for the 20 wt % POM blend the conversion will be less, but this indicates that the conversion did probably reach 60%, i.e., gelation. When the sample is cooled again at 10 °C/min (Figure 14c), spherulites start to grow again around 146 °C in the previous "spherulite-like" morphology. The nucleation of the spherulites starts at the same spot as for the isothermal crystallization at 140 °C. During the dynamic crystallization the spherulites continue to grow over the white borders visible in Figure 14b,c, indicating that the morphology in Figure 14 is built up by cured epoxy resin.

3.4. Spherulite Growth Rate Measurements. In this section, the influence of the phase separation on the spherulite growth rate will be studied under different circumstances. All data are summarized in Table 2. Four different crystallization conditions are used: (i) crystallization in blends which are fully cured at 180 °C, (ii) blends curing at 150 °C, (iii) blends curing at 145 °C, and (iv) blends without curing agent.

For the blends cured at 180 and 150 °C the isothermal crystallization occurs in the POM-rich phase after L−L demixing, which is not the case for those cured at 145 °C and for the uncured ones. The main difference, however, between the cure temperatures of 180 and 150 °C is that at 150 °C the cure process is still going on, while at 180 °C the isothermal crystallization occurs after full conversion. For both kinds of blends the spherulite growth rate could only be measured in those where the POM-rich phase forms the matrix. The data in Table 2 reveal a small increase in spherulitic growth rate with increasing concentration of POM for both blend types. However, almost 1 order of magnitude difference in growth rate can be observed between the two blend types. This gives us an indication of the composition of the POM-rich phase, since the crystallization temperature is the same. The smaller growth rate in the blends cured at 150 °C indicates that there has to be more epoxy resin present in the POM-rich phase (in monomer or oligomer form) compared to the blends cured at 180 °C. This can be explained as follows. Conversion measurements, using DSC, revealed a conversion degree of 33% for the blend with 20 wt % POM, at the onset of isothermal crystallization at 150 °C. This implies that the epoxy resin is still present in the oligomer form. It has been shown in the literature that after the onset of RIPS small epoxy molecules together with the amine are preferentially inside the thermoplastic-rich phase.[35−38] The high concentration of epoxy oligomers in the thermoplastic-rich phase results in a smaller growth rate of the POM spherulites, as it will be seen further on that the polymerization of the epoxy resin favors the spherulite growth rate. In the case of the blends fully cured at 180 °C, the epoxy resin present in the POM-rich phase will have a higher molar mass compared to $T_{cure} = 150$ °C, since the conversion reached almost 100%[20] in the former case (at $T_{cure} = 150$ °C, the cure reaction is still going on). This results in a larger growth rate of the POM spherulites in the POM-rich phase for the blends cured at 180 °C. For comparison, the spherulite growth rate of pure POM at 150 °C is 1.80 μm/s.

Next, blends crystallized at 145 °C will be discussed. As has been described in section 3.2, isothermal curing at 145 °C starts with the formation of spherulites in the homogeneous sample. Later on, interspherulitic reaction-induced phase separation starts, evolving from a cocontinuous structure toward particle/matrix or phase-inverted structures, depending on the blend composition. Because the crystallization continues in the phase-separated structure (and consequently stops the phase separation process), the spherulites can be divided into three different zones. These different phase morphology types will moreover result in different spherulite growth rates. However, even during crystallization in the homogeneous blend, thus before phase separation starts, an increase in spherulite growth rate can already be observed. Figure 15 shows the growth rate of the

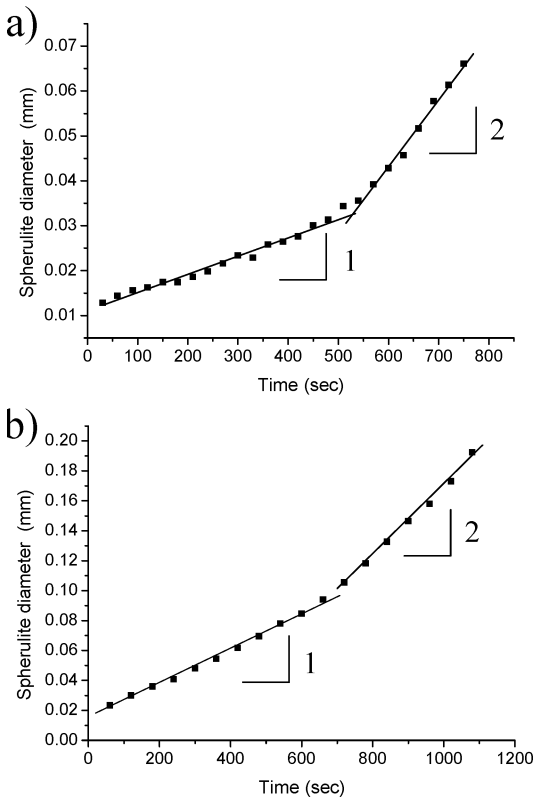

Figure 15. Graphs of the evolution of the diameter of a spherulite as a function of time in a blend with (a) 10 wt % POM and (b) 30 wt % POM during isothermal crystallization at 145 °C in the homogeneous blend system.

spherulites in the blends with 10 (Figure 15a) and 30 wt % POM (Figure 15b) cured at 145 °C before the onset of phase separation. In these graphs the increase of the spherulite diameter is plotted as a function of time. For both blend compositions an increase of the growth rate is observed. Also for the other blend compositions this trend is seen, which has been pointed to in Table 2 as "iso 145 °C before PS (1) and (2)". These numbers correspond to the numbers in Figure 15: PS(1) points to the spherulite growth at low conversions, and PS(2) points to the growth at higher conversion but still in the homogeneous sample. During the crystallization at 145 °C the epoxy resin is curing, which results in an increase of the average molar mass of the resin. The measurements mentioned above hence imply that the curing of the epoxy favors the isothermal crystallization of POM. This increase of the crystallization rate because of curing the epoxy resin has been observed before.[21] An explanation of this sudden increase can be found in the melting point depression caused by the epoxy resin, which acts like a solvent. At the start of the isothermal crystallization the conversion degree is very low and a large melting point depression is expected. While curing, the conversion degree increases, and as a consequence, the melting point depression becomes lower due to the increase of the molar mass of the epoxy resin. This smaller melting point depression results in a larger supercooling, and as a result, the spherulites will start growing faster. The sudden increase in the growth rate is situated around 20% of epoxy conversion. Table 2 also indicates an increase of the spherulitic growth rate with increasing concentration of POM, as expected.

After phase separation sets in, following observations are made concerning the spherulite growth rate. RIPS in the interspherulitic zone occurs via the spinodal demixing mechanism for all the considered blend compositions, i.e., 5 up to 30 wt % POM. The formed cocontinuous structure will respectively break up in a particle/matrix structure for the 5 and 10 wt % POM blends or in a phase-inverted structure for the blends with 15 up to 30 wt % POM. Compared to the homogeneous blends, an increase of the growth rate in the cocontinuous structures can be observed for all the blend compositions (Table 2). In the cocontinuous phase morphology a continuous POM-rich phase is present with a higher concentration of POM compared to the homogeneous sample. Concerning the growth rate in the more evolved phase-separated structures a difference has to be made between blends having a particle/matrix structure and those with a phase-inverted structure.

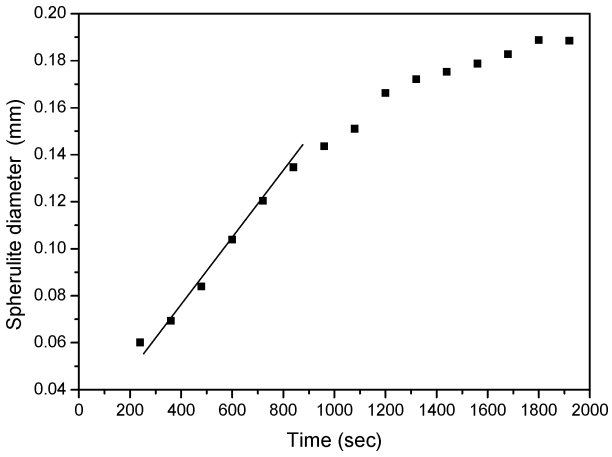

Figure 16. Graph of the evolution of the diameter of a spherulite as a function of time in a blend with 5 wt % POM during isothermal crystallization at 145 °C after RIPS has set in.

For the blends with 5 and 10 wt % POM, a decrease and final stop of the spherulite growth rate are observed when the spherulite enters the particle/matrix morphology. Indeed, in the particle/matrix structure the largest part of POM is dispersed in small droplets, and consequently only very little POM is present in the epoxy-rich matrix. When the spherulite growth front enters the particle/matrix structure, the crystallization will proceed due to the (slow) diffusion of the POM molecules toward the growth front, dissolved in the epoxy matrix. But at a certain time, the viscosity of the epoxy-rich phase will become too high and prevents further diffusion of POM. As a result, the spherulite growth will completely stop. Figure 16 shows the growth of a spherulite in a blend with 5 wt % POM in the phase-separated structure when cured at 145 °C. A clear decrease of the growth rate can be observed after more or less 18 min after the onset of RIPS. This coincides with the point where the spherulite enters the particle/matrix structure. The same trend has been observed for a blend with 10 wt % POM. For the blends with 15 up to 30 wt % POM, the cocontinuous structure evolves toward a phase-inverted structure where the POM-rich phase forms the matrix. For these blend compositions no change (or a very small increase) in the growth rate was detected, since the spherulites can grow easily both in the cocontinuous phase as in the phase-inverted structure; in both phase morphologies a POM-rich continuous phase is present.

The blends without DDS display a spherulite growth rate one order in magnitude smaller than that of the blends cured at 145 °C. The presence of unreacted epoxy monomer is very unfavorable for the growth of the spherulites because the epoxy monomers act like a solvent.

4. Conclusions

The competition between reaction-induced phase separation and isothermal crystallization has been studied for DGEBA/

POM/DDS blends at cure temperatures of 150, 145, and 140 °C. OM and SALLS measurements showed that isothermal crystallization starts after the onset of RIPS in the POM-rich matrix, when a cure temperature of 150 °C is applied. The phase morphologies are similar to those obtained at $T_{cure} = 180$ °C. When the blends are cured at 145 °C, the order of both processes is reversed: spherulitic crystallization starts before RIPS. At 145 °C, the phase morphologies are dominated by the POM spherulites. The higher the amount of POM, the faster the spherulites were formed and the smaller the phase-separated zone became. The thermal history of the blends proved to be crucial in the occurrence of RIPS since increasing the nucleation density could suppress the interspherulitic demixing. Moreover, the intraspherulitically segregated epoxy resin continued to cure, generating a "spherulite-like" morphology. Curing at 140 °C resulted in completely volume-filling spherulites without the occurrence of L−L phase separation due to the high nucleation density and high growth rate. The above-mentioned spherulite-like morphology was also observed.

The spherulite growth rate at 150 and 145 °C has been determined for blends cured for 4 h at 180 °C, for blends cured isothermally at 150 and 145 °C, and finally for blends without DDS hardener. Blends without DDS display the lowest growth rates, compared to the cured blends, which indicates that the polymerization of the epoxy monomers favors the spherulite growth. Also, the higher growth rates in the fully cured blends, compared to the blends curing at 150 or 145 °C, and the increase of the growth rate in the homogeneous blends at 145 °C, point to the favorable effect of the cure process. The increase of the growth rate has been attributed to the increase of the supercooling due to the decrease of the melting point depression caused by the polymerization of the epoxy resin. The phase morphology of the interspherulitic region, generated at $T_{cure} = 145$ °C, also plays an important role: particle/matrix structures stop the spherulite growth, whereas phase-inverted structures enhance the spherulite growth rate compared to the homogeneous samples.

Acknowledgment. The authors acknowledge the Fund for Scientific Research Flanders, Belgium, for the financial support of this research. S. Goossens is indebted to the Institute for the Promotion of Innovation through Science and Technology (IWT-Flanders) for a research grant. S. Goossens thanks dr. B. Goderis for his help during the SALLS measurements.

References and Notes

(1) Williams, R. J. J.; Rozenberg, B. A.; Pascault, J. P. *Adv. Polym. Sci.* **1997**, *128*, 95−156.
(2) Girard-Reydet, E.; Sautereau, H.; Pascault, J. P.; Keates, P.; Navard, P.; Thollet, G.; Vigier, G. *Polymer* **1998**, *39*, 2269−2279.
(3) Ishii, Y.; Ryan, A. J. *Macromolecules* **2000**, *33*, 158−166.
(4) Okada, M.; Sun, J.; Tao, J.; Chiba, T.; Nose, T. *Macromolecules* **1995**, *28*, 7514−7518.
(5) Oyanguren, P. A.; Galante, M. J.; Andromaque, K.; Frontini, P. M.; Williams, R. J. J. *Polymer* **1999**, *40*, 5249−5255.
(6) Yoon, T.; Kim, B. S.; Lee, D. S. *J. Appl. Polym. Sci.* **1997**, *66*, 2233−2242.
(7) Bonnet, A.; Pascault, J. P.; Sautereau, H.; Taha, M.; Camberlin, Y. *Macromolecules* **1999**, *32*, 8517−8523.
(8) Maugey, J.; Van Nuland, T.; Navard, P. *Polymer* **2001**, *42*, 4353−4366.
(9) Inoue, T. *Prog. Polym. Sci.* **1995**, *20*, 119−153.
(10) Vanden Poel, G.; Goossens, S.; Goderis, B.; Groeninckx, G. *Polymer* **2005**, *46*, 10758−10771.
(11) Yamanaka, K.; Inoue, T. *Polymer* **1989**, *30*, 662−667.
(12) Kim, B. S.; Chiba, T.; Inoue, T. *Polymer* **1995**, *36*, 67−71.
(13) Chen, J. L.; Chang, F. C. *Macromolecules* **1999**, *32*, 5348−5356.
(14) Läuger, J.; Lay, R.; Maas, S.; Gronski, W. *Macromolecules* **1995**, *28*, 7010−7015.
(15) Zhang, J. N.; Zhang, Z. L.; Zhang, H. D.; Yang, Y. L. *Phys. Rev. E* **2001**, *64*, Art. No 051510.
(16) Wang, M.; Yu, Y.; Wu, X.; Li, S. *Polymer* **2004**, *45*, 1253−1259.
(17) Tao, Q.; Gan, W.; Yu, Y.; Wang, M.; Tang, X.; Li, S. *Polymer* **2004**, *45*, 3505−3510.
(18) Yu, Y.; Wang, M.; Gan, W.; Tao, Q.; Li, S. *J. Phys. Chem. B* **2004**, *108*, 6208−6215.
(19) Tanaka, H. *J. Phys.: Condens. Matter* **2000**, *12*, 207−264.
(20) Goossens, S.; Goderis, B.; Groeninckx, G. *Macromolecules* **2006**, *39*, 2953−2963.
(21) Guo, Q.; Groeninckx, G. *Polymer* **2001**, *42*, 8647−8655.
(22) Guo, Q.; Harrats, C.; Groeninckx, G.; Reynaers, H.; Koch, M. H. J. *Polymer* **2001**, *42*, 6031−6041.
(23) Kulshreshtha, B.; Ghosh, A. K.; Misra, A. *Polymer* **2003**, *44*, 4723−4734.
(24) Kulshreshtha, B.; Ghosh, A. K.; Misra, A. *J. Macromol. Sci., Phys.* **2003**, *B42*, 307−323.
(25) Schut, J.; Stamm, M.; Dumon, M.; Galy, J.; Gérard, J. F. *Macromol. Symp.* **2003**, *202*, 25−35.
(26) Salmon, N.; Carlier, V.; Schut, J.; Remiro, P. M.; Mondragon, I. *Polym. Int.* **2005**, *54*, 667−672.
(27) Guo, Q.; Harrats, C.; Groeninckx, G.; Koch, M. H. J. *Polymer* **2001**, *42*, 4127−4140.
(28) Guo, Q.; Peng, X.; Wang, Z. *Polymer* **1991**, *32*, 53−57.
(29) Lu, H.; Zheng, S. X. *Polymer* **2003**, *44*, 4689−4698.
(30) Zheng, S. X.; Guo, Q. P.; Mi, Y. L. *Polymer* **2003**, *44*, 867−876.
(31) Guo, Q. P.; Slavov, S.; Halley, P. J. *J. Polym. Sci., Part B: Polym. Phys.* **2004**, *42*, 2833−2843.
(32) Swier, S.; Van Assche, G.; Vuchelen, W.; Van Mele, B. *Macromolecules* **2005**, *38*, 2281−2288.
(33) Inaba, N.; Yamada, T.; Suzuki, S.; Hashimoto, T. *Macromolecules* **1988**, *21*, 407−414.
(34) Goossens, S. Micro- and Nanostructured thermoplastic/thermosetting Polymer Blend Systems: Reaction-Induced Phase Separation, Crystallization and Morphology. PhD Thesis KULeuven, Belgium, 2006; Chapter 6, pp 151−178.
(35) Oyanguren, P. A.; Riccardi, C. C.; Williams, R. J. J.; Mondragon, I. *J. Polym. Sci., Part B: Polym. Phys.* **1998**, *36*, 1349−1359.
(36) Clarke, N.; McLeish, T. C. B.; Jenkins, S. D. *Macromolecules* **1995**, *28*, 4650−4659.
(37) Riccardi, C. C.; Borrajo, J.; Williams, R. J. J. *Polymer* **1994**, *35*, 5541−5550.
(38) van Overbeke, E.; Devaux, J.; Legras, R.; Carter, J. T.; McGrail, P. T.; Carlier, V. *Polymer* **2003**, *44*, 4899−4908.

MA061415T